Microarray and Proteomic Analysis of Breast Cancer Cell and Osteoblast Co-cultures

ROLE OF OSTEOBLAST MATRIX METALLOPROTEINASE (MMP)-13 IN BONE METASTASIS*⑤

Charlotte Morrison[‡§1]**, Stephanie Mancini**[¶1]**, Jane Cipollone**[¶]**, Reinhild Kappelhoff**[‡§]**, Calvin Roskelley**[¶]**, and Christopher Overall**[‡§‖2]

From the ‡Centre for Blood Research and Departments of §Oral Biological and Medical Sciences, ‖Biochemistry and Molecular Biology, and ¶Cellular and Physiological Sciences, University of British Columbia, Vancouver, British Columbia V6T 1Z3, Canada

Dynamic reciprocal interactions between a tumor and its microenvironment impact both the establishment and progression of metastases. These interactions are mediated, in part, through proteolytic sculpting of the microenvironment, particularly by the matrix metalloproteinases, with both tumors and stroma contributing to the proteolytic milieu. Because bone is one of the predominant sites of breast cancer metastases, we used a co-culture system in which a subpopulation of the highly invasive human breast cancer cell line MDA-MB-231, with increased propensity to metastasize to bone, was overlaid onto a monolayer of differentiated osteoblast MC3T3-E1 cells in a mineralized osteoid matrix. CLIP-CHIP® microarrays identified changes in the complete protease and inhibitor expression profile of the breast cancer and osteoblast cells that were induced upon co-culture. A large increase in osteoblast-derived MMP-13 mRNA and protein was observed. Affymetrix analysis and validation showed induction of MMP-13 was initiated by soluble factors produced by the breast tumor cells, including oncostatin M and the acute response apolipoprotein SAA3. Significant changes in the osteoblast secretomes upon addition of MMP-13 were identified by degradomics from which six novel MMP-13 substrates with the potential to functionally impact breast cancer metastasis to bone were identified and validated. These included inactivation of the chemokines CCL2 and CCL7, activation of platelet-derived growth factor-C, and cleavage of SAA3, osteoprotegerin, CutA, and antithrombin III. Hence, the influence of breast cancer metastases on the bone microenvironment that is executed via the induction of osteoblast MMP-13 with the potential to enhance metastases growth by generating a microenvironmental amplifying feedback loop is revealed.

Metastasis, the complex multistep process by which primary tumors establish growth at distant secondary sites, is the major cause of mortality in cancer. In breast cancer, metastasis to bone is one of the most common sites for secondary tumor growth. Although most of secondary breast cancer lesions ultimately become osteolytic, the underlying molecular mechanisms and bone-tropic factors that promote initial tumor cell homing to, and establishment within, the bone microenvironment are not well understood.

A number of studies have established "metastatic signatures" for breast cancer cells by comparing highly invasive cell lines such as MDA-MB-231 (MDA-231) to noninvasive lines such as MCF-7, both at the gene expression and proteome level (1). Such transcriptomic studies have identified organ-specific metastatic signatures through repetitive *in vivo* passaging of MDA-231 breast cancer cells (2, 3). The metastatic signature identified for a bone homing variant MDA-MB-231–1833/TR (MDA-1833) encompasses increased expression of a functionally diverse set of mRNAs, including matrix metalloproteinase (MMP)[3] 1 (also known as tissue collagenase), the chemokine receptor CXCR4, connective tissue growth factor, interleukin (IL)-11, and osteopontin (4). The combined overexpression of three of these molecules (osteopontin, IL11, and CXCR4 or connective tissue growth factor or MMP-1) in the parental MDA-231 was required to achieve the same level of bone metastasis, indicating that multiple interactions are involved in promoting bone metastasis. Nonetheless, these approaches only consider the contribution of the tumor cells and not the cells of the bone microenvironment. Hence, the consequences of increased expression of these signature molecules at the protein level and subsequent reciprocal responses of the resident osteoblasts remain undefined.

The microenvironment of the tumor greatly impacts both the establishment and progression of metastases and involves dynamic and reciprocal interactions between stroma and tumor. For example, in bone metastasis, a "vicious cycle" is established between the tumor and bone-derived cells (osteoblasts and osteoclasts). Tumor-derived factors induce osteoblast-mediated recruitment and differentiation of lytic oste-

⌘ *Author's Choice*—Final version full access.
⑤ The on-line version of this article (available at http://www.jbc.org) contains supplemental Tables 1–11 and Figs. 1 and 2.
[1] Both authors contributed equally to this work.
[2] Supported by a Canada Research Chair in Metalloproteinase Proteomics and Systems Biology. To whom correspondence should be addressed: Centre for Blood Research, University of British Columbia, 2350 Health Sciences Mall, Vancouver, British Columbia V6T 1Z3, Canada. E-mail: chris.overall@ubc.ca.

[3] The abbreviations used are: MMP, matrix metalloproteinase; QRT, quantitative RT; Tricine, *N*-[2-hydroxy-1,1-bis(hydroxymethyl)ethyl]glycine; BH, Benjamini and Hochberg; OSMR, OSM receptor; MMPI, MMP inhibitor; RANK, receptor-activator of nuclear factor-κB; RANKL, RANK ligand; PDGFR, PDGF receptor; OPG, osteoprotegerin.

oclasts via receptor-activator of nuclear factor-κB (RANK)/RANK ligand (L) pathways, thereby promoting osteoclast-driven destruction of bone and the release of pro-tumorigenic factors. Although the RANK/RANKL pathway is a focus of considerable research as a potential therapeutic target (5, 6), it is clear that other molecules and pathways are involved in promoting the establishment of bone metastasis, and identifying these pathways may lead to alternative therapeutic targets. Such pathways are in part mediated or regulated through the expression of proteases and proteolytic modulation of the microenvironment, with both tumors and stroma contributing to the proteolytic milieu. The cellular origin of proteases and their regulators is, however, not always clear. To unravel these interactions, global approaches are needed, as individual proteases do not act alone but function as part of a network, the "protease web" (7), and are regulated by a myriad of other proteins such as activators, inhibitors, co-factors, receptors, substrates, and cleavage products.

One family of proteases, the zinc-dependent endopeptidases MMPs, have been shown to play a pivotal role in tumor metastasis through modulation of tumor growth, angiogenesis, and invasion (8). Many of the MMPs are expressed in breast cancer (9); they are frequently included in metastatic signatures (2–4) and have been implicated in facilitating metastasis to bone (10). In the past, it has been assumed that because MMP expression levels are elevated in cancer, MMPs have detrimental effects and therefore must be drug targets. However, both pathological and beneficial roles for MMPs in cancer are now recognized (7). The first example of anti-tumorigenic MMP activity was described for MMP-8 where genetic deficiency dramatically increases skin carcinoma (11). In *Mmp14*-deficient mice, breast cancer tumors develop faster than in their wild type counterparts but show a 50% reduction in metastasis (12). The reverse is true for *Mmp11* deficiency (13–15). These studies highlight the need to carefully dissect the role of a given MMP in a particular cancer and, through the identification of substrates, thereby define function in a site-specific context (16). Distinguishing between substrates and pathways that have detrimental *versus* beneficial effects in cancer may lead to the identification of successful novel drug targets as well as anti-targets that must be avoided in therapy or else risk worsening the disease (7).

MMP-13 (collagenase-3) was first cloned from a breast cancer tumor (17) and has since been shown to be elevated in a variety of other cancers (18, 19). In addition, in xenograft mouse models of breast cancer, induction of MMP-13 in tumor-associated stroma was demonstrated (20). MMP-13 also plays a crucial role in normal bone development as revealed by the phenotype of $Mmp13^{-/-}$ mice, which have severe abnormalities in skeletal development (21, 22). Multiple induction pathways have been demonstrated for MMP-13 (23–27), which is secreted as an inactive zymogen, that *in vitro* is activated by MMP-2 and MMP-14 (28). The ability of MMP-13 to cleave a variety of extracellular matrix molecules and associated proteins *in vitro,* such as collagen, tenascin, decorin, biglycan, and aggrecan (29–32), has been extensively studied. MMP-13 has also been shown to process a number of other proteins *in vitro,* including chemokines (33, 34), adhesion molecules such as

intercellular adhesion molecule 1 (35), and growth factors such as connective tissue growth factor (36) and TGF-β (37), all of which may affect tumor cell homing. Modifying the function of bioactive substrates has great potential in altering the course of metastatic disease by signaling pathway perturbations. However, despite the abundant evidence linking elevated MMP-13 expression and breast cancer, the substrate repertoire of MMP-13 in this scenario is not well characterized. Our goal was to study the interactions between differentiated osteoblast MC3T3-E1 cells and MDA-231 breast cancer cell lines to identify osteoclast *independent* interactions that are important in promoting bone metastasis.

EXPERIMENTAL PROCEDURES

Cell Culture—MC3T3-E1 mouse osteoblast cells were seeded at high density (1×10^5 cells/cm^2 in 6-well plates or for proteomic experiments, 10-cm^2 culture dishes) in growth medium (α-minimal essential medium with 10% fetal bovine serum). After overnight incubation at 37 °C, osteoblastic differentiation medium was added (growth medium with 10 mM β-glycerophosphate and 25 μM ascorbic acid). The differentiation medium was changed every 2 days, and the cells were grown for a week during which alkaline phosphatase and von Kossa staining were used to demonstrate the differentiation of the MC3T3-E1 cells and the mineralization of the extracellular matrix secreted by the cells, respectively (38). Breast cancer cells MDA-231 and a subpopulation, 1833 (MDA-1833), were then seeded at 1×10^5 cells/cm^2 in differentiation medium in 6-well plates or added to the 6-well plates containing differentiated MC3T3-E1 cells or onto Transwell inserts with 1-μm filters positioned over the MC3T3-E1 cells. After 6 h when the MDA-231/1833 cells had adhered, the cells were gently washed three times with 2 ml of α-minimal essential medium without serum, and 1 ml of serum-free α-minimal essential medium was then added. Other wells containing MC3T3-E1 cells were maintained without the addition of breast cancer cells; these were washed and incubated serum-free (as above) or grown with 1 ml of 24-h conditioned medium (serum-free) from MDA-1833 cells. For MMP-13 activation assays, 100 μg/ml concanavalin A was added (39). In other experiments, MDA-1833 cell-conditioned medium or 10 ng/ml oncostatin M (OSM) (R&D Systems Inc.) was added to MC3T3-E1 in the presence or absence of 20 μM JAK-1 inhibitor (Calbiochem) or 5 μg/ml anti-gp130 antibody (MAB4682) (R&D Systems Inc.). The cells were then cultured for 24 h followed by harvesting of supernatants and lysing of cells for RNA extraction. Two technical replicates were done for each culture condition, and three biological replicates were performed in total.

Microarray Analysis—Using RNeasy (Qiagen), RNA was extracted from MC3T3-E1, MDA-231, and MDA-1833 cells that had been cultured alone or co-cultured together with indirect contact using filters, and MC3T3-E1 cultured in the presence of MDA-1833 cell-conditioned medium. Preparation of RNA samples for CLIP-CHIP® analysis was performed as described previously (40). The microarrays were scanned using Imagene software, and statistical analysis was performed using CARMAweb software (41). Microarrays were normalized using normexp for background and print-tip loess for within

array and quantile for between array corrections. For co-cultured cells, a paired moderated t test using linear models for microarray (Limma) was used to determine differentially expressed genes based on expression values, and false discovery rates were controlled using Benjamini and Hochberg (BH) adjusted p values (<0.05). Three independent co-culture experiments were analyzed with duplicate samples for each culture condition. Each sample was analyzed using a CLIP-CHIP microarray slide that contains two copies of the array. For Affymetrix microarray analysis, samples were labeled using a one-cycle labeling kit and hybridized to Gene-Chip® Mouse Genome 430 Plus 2.0 microarrays (Affymetrix Inc.). Statistical parameters were calculated using the MAS 5 algorithm. Quantile normalization was used, and gene expression intensities were calculated using the Robust Multichip Average algorithm. Differentially expressed genes were identified using Bayes moderated t-statistics, and false discovery rates were controlled using BH-adjusted p values (< 0.05). Only mRNAs with a >2-fold change in expression were reported.

QRT-PCR—RNA samples from MC3T3-E1 cells co-cultured with MDA-1833 cells or incubated with MDA-1833 cell-conditioned medium or OSM or anti-gp130 antibody were analyzed by QRT-PCR. The DNase I-treated RNA (1 μg/sample) was reverse-transcribed using the cDNA kit (Applied Biosystems). QRT-PCR using the 7500 Fast Real Time PCR system (Applied Biosystems) was performed on 20 ng of cDNA using TaqMan gene expression assays (Applied Biosystems). The following expression analysis kits were used for murine MMP-13 (Mm00439491_m1): MMP-2 (Mm00439508_m1) and MMP-14 (Mm00485054_m1), OSMR (Mm00495424_m1), and gp130 (Mm00439668_m1). TaqMan ribosomal RNA control reagent was used as an 18 S internal control for all samples, and the QRT-PCR results were normalized to this control. Samples and standards were assayed in duplicate, and the relative RNA levels in MC3T3-E1 cells co-cultured with MDA-231 or MDA-1833 cells or MDA-1833 cell-conditioned medium were compared with the control cells grown alone under serum-free conditions.

Western Blot Analysis of MC3T3-E1 and MDA-1833 Cultures—MC3T3-E1 cells co-cultured with MDA-1833 cells or incubated with MDA-1833 cell-conditioned medium or OSM or anti-gp130 antibody were concentrated 10-fold by precipitation with TCA (10% final) and analyzed by Western blotting using the following antibodies: anti-MMP-13 (MAB13426) at 0.5 μg/ml (Millipore); anti-MMP-2 at 0.5 μg/ml (42); anti-OSMR (AF662) at 0.2 μg/ml (R&D Systems Inc.); anti-gp130 (06-291) at 2 μg/ml (Millipore), and anti-actin (A4700) at 1:5000 dilution (Sigma). A PhosphoPlus® Stat3 (Tyr-705) antibody kit (9130) (Cell Signaling Technology) was used to analyze MC3T3-E1 cell extracts. MDA-1833 supernatants were analyzed with the following: anti-OSM (MAB295) at 2 μg/ml; anti-LIF (MAB250) at 2 μg/ml), and anti-IL6 (AF-206-NA) at 0.2 μg/ml (R&D Systems Inc.). Secondary antibodies goat anti-mouse or rabbit Alexa 680 (Invitrogen) were used at 10 μg/ml, and proteins were visualized using an Odyssey detector (Li-COR). Zymography using 8% polyacrylamide gels (43) was also used to detect the endogenous MMP-2 in MC3T3-E1 cells.

Recombinant Proteins—Recombinant C-terminally FLAG-tagged human MMP-13 was expressed in Chinese hamster ovary cells and purified from culture supernatants using two columns. First, 2 liters of culture supernatant was passed over a green-agarose column (Sigma) (V_t = 20 ml), and the column was then washed with $10\times V_t$ MES buffer (50 mM MES, 100 mM NaCl, 5 mM CaCl$_2$, 0.02% NaN$_3$, pH 6). Bound protein was eluted using MES buffer containing 1 M NaCl, and fractions containing MMP-13 were pooled and dialyzed into Tris-buffered saline (TBS), pH 7.2. MMP-13 was then purified to homogeneity using an anti-FLAG-agarose column (V_t = 2 ml) (Sigma) and was eluted from the column in 100 mM glycine, pH 3.5, followed by dialysis into HEPES buffer (50 mM HEPES, 150 mM NaCl, pH 7.2).

The cDNA for murine serum amyloid (SAA) 3 was cloned into the PET28b expression vector and used to transform BL21 Gold *Escherichia coli*. His-tagged SAA3 protein was purified to homogeneity from the cytoplasmic fraction of a 1-liter culture using a Ni^{2+}-chelate column (V_t = 5 ml). Bound protein was eluted in buffer containing 50 mM Tris, 150 mM NaCl, 400 mM imidazole, pH 7.5, and fractions containing SAA3 were pooled and dialyzed into HEPES buffer. SAA3 was analyzed by silver-stained SDS-PAGE, Western blotting using an anti-SAA3 antibody (kindly provided by Dr. P. Scherer, Albert Einstein College of Medicine) (44), and an anti-His antibody (Qiagen). The molecular mass was determined by matrix-assisted laser desorption ionization (MALDI)-time of flight (TOF) mass spectrometry (MS) using a Voyager-DE STR biospectrometry work station (Applied Biosystems Inc.).

CCL2 and CCL7 chemokines were synthesized as described previously (34, 45), and recombinant platelet-derived growth factor (PDGF)-C (R&D Systems Inc.), antithrombin III (Affinity Bioreagents), osteoprotegerin (Cell Sciences), and CutA (Abcam) were purchased.

Proteomic Sample Preparation and iTRAQ Labeling—MC3T3-E1 cells were cultured in 10-cm^2 dishes in differentiation medium as described for 7 days and then washed three times with serum-free medium and incubated for 48 h in 8 ml of serum-free medium with and without 0.1 or 1 μg/ml recombinant active MMP-13. Supernatants were harvested, and PMSF (0.1 mM final) and EDTA (1 mM final) were added. After centrifugation (600 $\times$ g, 10 min) 20-ml supernatants were precipitated with TCA (10% final) to concentrate protein, and protein pellets were resuspended in 2 ml of HEPES buffer with 0.05% SDS, pH 7.2, and protein concentration was determined using the BCA assay (Pierce). Tryptic digestion of 100 μg of protein for each condition and differential labeling of peptides with iTRAQ reagents (Applied Biosystems) was performed as described previously (46). Untreated control samples were labeled with the 114 isobaric tag. Sample preparation and two-dimensional LC MS/MS analysis using a QStar Pulsar Quadrupole TOF mass spectrometer (Applied Biosystems/Sciex) were as described previously (46).

Proteomic Data Analysis—ProteinPilot (Version 1.0) (Applied Biosystems) was used for protein identification and quantification after searching against the mouse IPI version 3.28 data base appended with human MMP-13. A confidence cutoff for protein identification >95% was applied, and biolog-

ical modifications were included in the identification. The intensity of the 114, 115, 116, and 117 atomic mass unit signature mass tags generated upon MS/MS fragmentation from the iTRAQ-labeled tryptic peptides were used to quantify the relative levels of peptides and hence proteins in each sample. To determine the relative abundance of proteins in MMP-13-treated cells *versus* untreated controls, peptide and protein ratios were expressed using the 114 tag used to label control samples as the denominator.

Substrate Validation—To validate MMP-13 substrates biochemically, 20-μl reactions of 1 μg of recombinant protein with MMP-13 (molar ratios of enzyme/substrate ranging from 1:100 to 1:10) in HEPES buffer were incubated at 37 °C for 16 h. Controls included substrate incubated alone or with MMP-13 in the presence of 10 μM of the MMP inhibitor (MMPI) marimastat synthesized as described previously (47). Cleavage assays (10 μl diluted 1:2 in SDS-PAGE loading buffer) were analyzed by SDS-PAGE using 15% Tris-glycine or 10% Tris-Tricine gels and silver staining or Western blot analysis with the antibodies listed above and the following: anti-PDGF-C (R&D Systems Inc.), anti-phospho-ERK1/2, and anti-ERK1/2 (Cell Signaling Technologies). Where indicated, the masses of proteins and cleavage products were determined by MALDI-TOF MS.

RESULTS

CLIP-CHIP Microarray Analysis of Co-cultured Breast Cancer and Osteoblast Cell Lines—We determined the dynamic bidirectional interactions that might occur between breast cancer tumors and osteoblasts in the metastatic bone microenvironment. Human MDA MB-231 breast cancer cell lines were co-cultured on Transwell filters over differentiated mouse osteoblast MC3T3-E1 cells. This ensured that the two cell types were physically separated from one another such that we could identify the effects exerted by soluble paracrine factors produced by both the osteoblasts and tumor cells. As controls for basal expression levels, all three cell types were also cultured alone. Although human and mouse systems are not equivalent, utilizing human breast cancer cells and mouse osteoblasts aided in the clarification of the contribution of tumor and stroma and parallels well established human tumor xenograft mouse models of metastases (2, 3, 20).

Initially, using the CLIP-CHIP human arrays, we compared the protease and inhibitor mRNA profiles of MDA-231 and a subpopulation MDA-1833 that have increased propensity for metastasis to bone (see supplemental Fig. S1) (4). Our data confirmed the previously reported increase in expression of MMP-1 in the bone homing MDA-1833 subpopulation (4). In addition, 17 other proteases and 8 inhibitors had a 2-fold or greater change in expression in MDA-1833 cells compared with the parent cell line MDA-231. Notable differences in MDA-1833 with the potential to impact metastasis (48, 49) included an 8- and 16-fold reduction in the cysteine protease inhibitor cystatin E/M and serine protease inhibitor Kazal type 4 (SPINK4), respectively. We then analyzed MDA-1833 breast cancer cells co-cultured with MC3T3-E1, and this revealed small (<2-fold) but significant changes in the expression of six protease and inhibitor mRNAs (supplemental Table S1).

TABLE 1

CLIP-CHIP microarray analysis of the changes in the complete protease and inhibitor mRNA expression profile of MC3T3-E1 cells upon co-culture with MDA-MB-231 subpopulation 1833 (MDA-MB-1833) cells

Changes in mRNA expression are given as fold changes comparing MC3T3-E1 cells co-cultured *versus* grown alone. All changes are significant with BH-adjusted *p* values <0.05.

Differentially expressed mRNA in MC3T3 cells co-cultured with MDA-1833	-Fold change
Collagenase 3 (MMP-13)	5.9
Proteasome catalytic subunit 2i	2.0
PHEX endopeptidase	2.0
Carboxypeptidase X2	2.0
Caspase-12	2.0

Analysis of mRNA expression in MC3T3-E1 osteoblasts co-cultured with MDA-1833 cells identified five proteases with a 2-fold or greater change in expression (Table 1). The largest change observed in MC3T3-E1 cells upon culture with MDA-1833 was a $n \sim 6$-fold increase in MMP-13 mRNA expression. This specific elevation of MMP-13, but not MMP-2 or MMP-14 mRNA levels in MC3T3-E1 co-cultured cells, was confirmed by QRT-PCR analysis (Fig. 1*A*). MDA-231 also induced expression of MMP-13 in MC3T3-E1 cells (supplemental Table S2 and supplemental Fig. S2*A*).

Induction of MMP-13 was also observed by CLIP-CHIP (data not shown) and Affymetrix microarrays (Fig. 2*A*), and QRT-PCR analyses (Fig. 2*B*) when differentiated MC3T3-E1 cells were cultured in the presence of MDA-1833 cell-conditioned medium, confirming that a soluble factor produced by the breast cancer cells induced MMP-13 expression in the osteoblasts. We therefore focused our study on the novel up-regulation of MMP-13 in osteoblasts by breast cancer cells.

MMP-13 Protein Expression and Activation—The changes observed in the co-cultured MC3T3-E1 MMP-13 mRNAs were manifest at the protein level. Western blot analysis of MC3T3-E1 supernatants revealed an increase in MMP-13 protein when cultured with either MDA-1833 (Fig. 1*B*) or MDA-231 (supplemental Fig. S2*B*) cells grown in direct contact, separated by filters, or after addition of conditioned medium from the breast cancer cells. Interestingly, the MMP-13 retained the pro-domain and was not activated suggesting that the activating mechanism for MMP-13 was lacking in this particular co-culture system, which is less complex than the osteoblastic stroma *in vivo*. Regardless, to determine whether it was possible to achieve MMP-13 activation by MMP-14, a known MMP activator, MC3T3-E1 cells were co-cultured in direct contact with MDA-231 cells transfected for stable cell-surface expression of MMP-14 or catalytically inactive MMP-14 E240A as a control (supplemental Fig. S2*C*). Expression of MMP-14 by MDA-231 did not result in activation of MC3T3-E1-derived MMP-13. However, MMP-14 is expressed in the MC3T3-E1 cells before and after co-culture as revealed by CLIP-CHIP and Affymetrix microarray (data not shown), and if MC3T3-E1 were treated with concanavalin A in the presence of MDA-1833 cell-conditioned medium, to induce MMP-14 (39) and MMP-13 expression, respectively, both the 55-kDa pro-form and the 44-kDa activated form of MMP-13 were produced by the MC3T3-E1 (Fig. 1*C*). Concanavalin A also induced MMP-2 activation via MMP-14 and MMP-13 expression (Fig. 1*C*) but
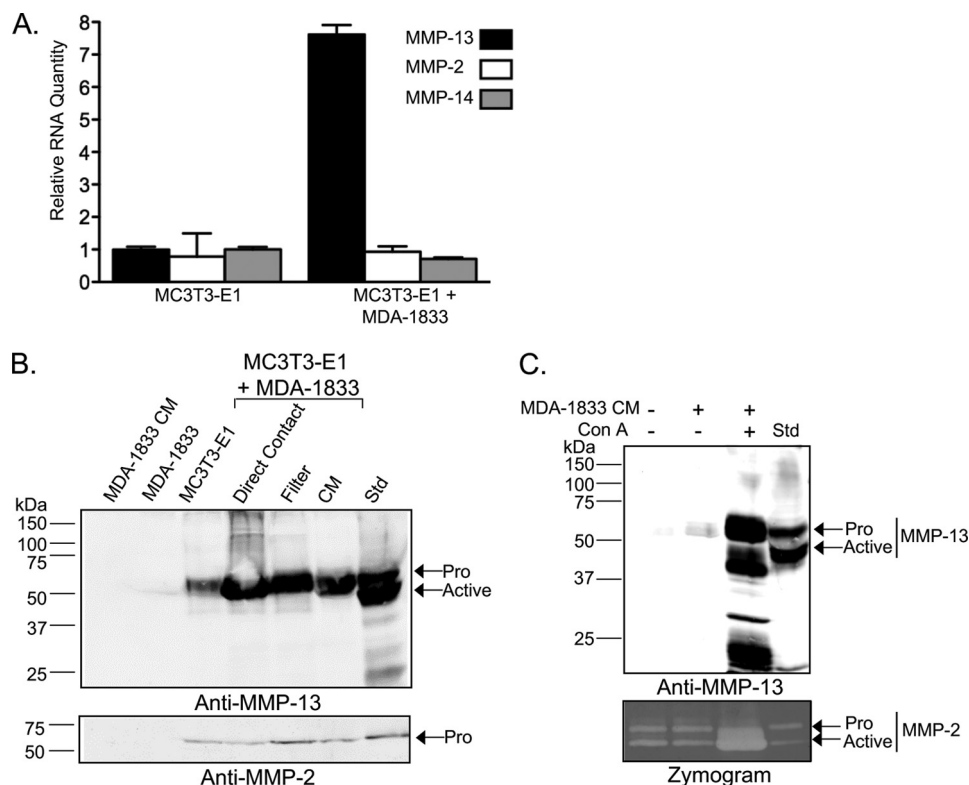
FIGURE 1. **MMP-13 induction, expression, and activation in MC3T3-E1 cells.** *A,* quantitative real time-PCR of MMP-13, MMP-2, and MMP-14 in MC3T3-E1 cells grown alone or co-cultured with MDA-1833 on Transwell filters. *B,* Western blot analysis of MMP-13 expression in MC3T3-E1 cell culture supernatants grown alone or co-cultured with MDA-1833 in direct contact, separated on Transwell filters, or after the addition of MDA-1833 cell-conditioned medium (*CM*). *C,* Western blot analysis of MMP-13 in MC3T3-E1 culture supernatants of cells grown in the presence of MDA-1833 cell-conditioned medium (*CM*) with and without concanavalin (*Con*) A. Western blot and gelatin zymograms of MMP-2 expression are included as controls. Standards (*Std*) are purified recombinant MMP-13 or MMP-2.

not activation (data not shown) as reported previously (39, 50). This would suggest that proximity between MMP-13 and MMP-14 is required for activation to occur. MMP-14 expression has been shown to be developmentally regulated during osteoblast differentiation (51–53). *In vivo*, elevated MMP-14 expression in the stroma of breast cancer tumors has been reported, and thus activation of tumor-induced stromal MMP-13 is likely to occur in the more complex *in vivo* microenvironmental milieu (54).
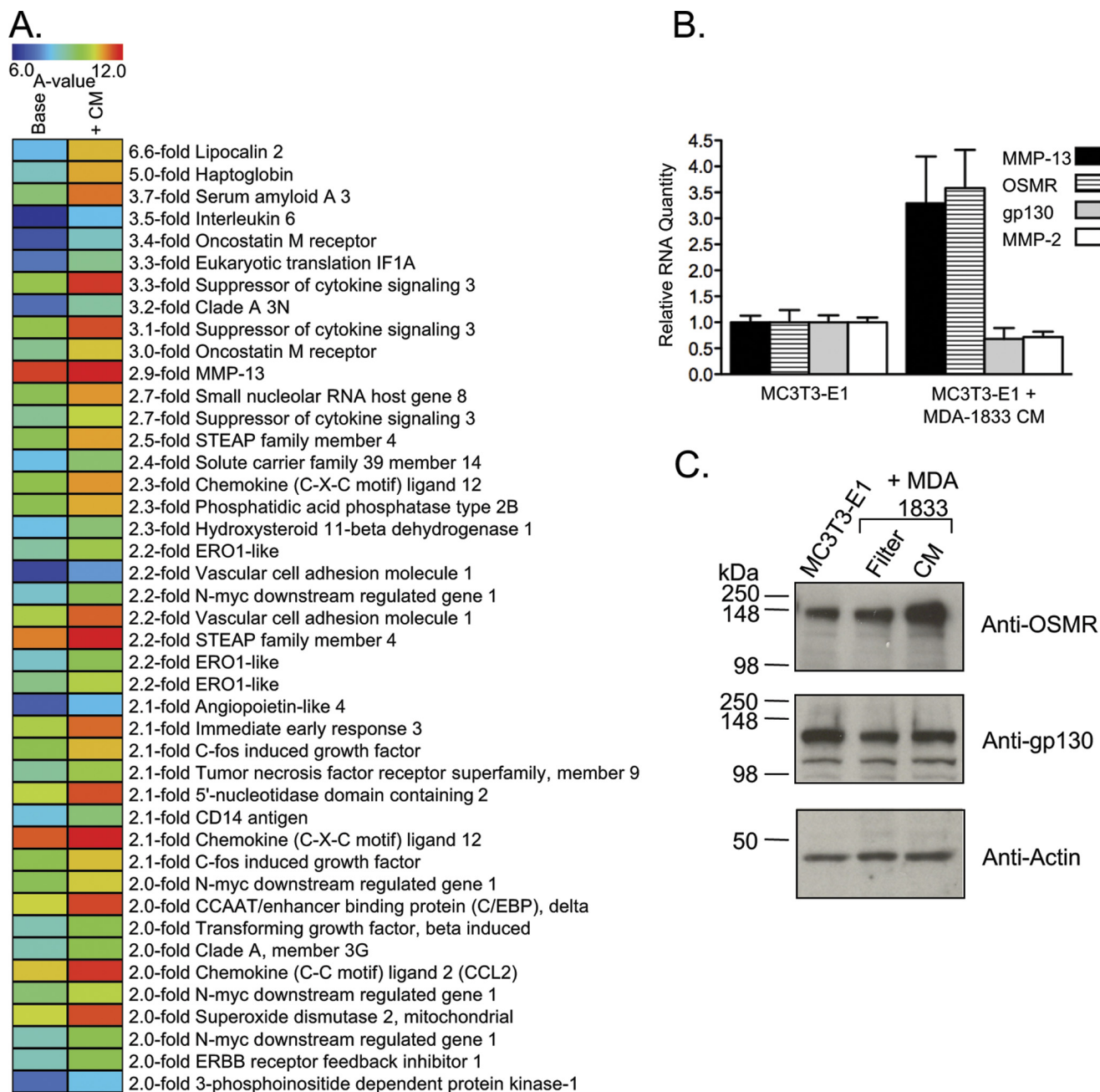
IL-6 Family Cytokines in the Tumor Cell-Osteoblast Microenvironment—Affymetrix microarray analysis was used to identify the microenvironmental signals that were potentially involved in the tumor cell-mediated MMP-13 up-regulation in osteoblasts. This analysis revealed a 3-fold increase in the expression of the ligand-binding subunit of the heterodimeric receptor for the IL-6 family cytokine oncostatin M (*i.e.* OSMR) in MC3T3-E1 osteoblasts after they were exposed to MDA-1833 tumor cell-conditioned medium (Fig. 2*A*; supplemental Table S3). This up-regulation was confirmed by QRT-PCR at the mRNA level (Fig. 2*B*) and by Western blotting at the protein level (Fig. 2*C*). Although there was no evidence that MDA-1833-conditioned medium increased levels of the second signaling subunit of the OSM receptor (*i.e.* gp130) in MC3T3-E1 osteoblasts, the mRNA and protein were both constitutively present (Fig. 2, *B* and *C*). The latter was not surprising given that gp130 is the common signaling subunit found in all IL-6 family cytokine receptors (55).

OSM and other IL6 family cytokines induce MMP-13 expression in primary cultures of fetal osteoblasts (23, 26). We confirmed that recombinant OSM induces MMP-13 mRNA and protein expression in MC3T3-E1 osteoblasts (Fig. 3, *A* and *C*), and we showed that it also induces OSMR subunit expression (Fig. 3*A*). Importantly, OSM as well as the IL-6 family cytokines LIF and IL-6 itself were all present in MDA-1833-conditioned medium (Fig. 3*B*). We also found that IL-6 mRNA was up-regulated in the MC3T3-E1 cells after incubation with MDA-1833 cell-conditioned media (Fig. 2*A*). This suggests that an IL-6 family cytokine feed-forward activation loop may exist in the tumor cell/osteoblast microenvironment.

All IL-6 family cytokines, including OSM, activate JAK/STAT3 signaling downstream of the common gp130 IL-6 receptor subunit (55). In chondrocytes and chondrosarcoma cells, this pathway transcriptionally up-regulates MMP-13 expression (56). We demonstrated that recombinant OSM and MDA-1833-conditioned medium both induced a JAK-dependent increase in STAT-3 phosphorylation in MC3T3-E1 osteoblasts (Fig. 3*D*). Importantly, pharmacological JAK inhibition greatly curtailed the ability of recombinant OSM and MDA-1833 cell-conditioned medium to induce STAT-3 phosphorylation and MMP-13 expression (Fig. 3*D*).

We were unable to prevent MDA-1833 cell-conditioned medium from increasing STAT-3 phosphorylation or MMP-13 expression in MC3T3-E1 osteoblasts using an OSM-blocking antibody (data not shown), which likely reflects the presence of

A.

6.6-fold Lipocalin 2
5.0-fold Haptoglobin
3.7-fold Serum amyloid A 3
3.5-fold Interleukin 6
3.4-fold Oncostatin M receptor
3.3-fold Eukaryotic translation IF1A
3.3-fold Suppressor of cytokine signaling 3
3.2-fold Clade A 3N
3.1-fold Suppressor of cytokine signaling 3
3.0-fold Oncostatin M receptor
2.9-fold MMP-13
2.7-fold Small nucleolar RNA host gene 8
2.7-fold Suppressor of cytokine signaling 3
2.5-fold STEAP family member 4
2.4-fold Solute carrier family 39 member 14
2.3-fold Chemokine (C-X-C motif) ligand 12
2.3-fold Phosphatidic acid phosphatase type 2B
2.3-fold Hydroxysteroid 11-beta dehydrogenase 1
2.2-fold ERO1-like
2.2-fold Vascular cell adhesion molecule 1
2.2-fold N-myc downstream regulated gene 1
2.2-fold Vascular cell adhesion molecule 1
2.2-fold STEAP family member 4
2.2-fold ERO1-like
2.2-fold ERO1-like
2.1-fold Angiopoietin-like 4
2.1-fold Immediate early response 3
2.1-fold C-fos induced growth factor
2.1-fold Tumor necrosis factor receptor superfamily, member 9
2.1-fold 5'-nucleotidase domain containing 2
2.1-fold CD14 antigen
2.1-fold Chemokine (C-X-C motif) ligand 12
2.1-fold C-fos induced growth factor
2.0-fold N-myc downstream regulated gene 1
2.0-fold CCAAT/enhancer binding protein (C/EBP), delta
2.0-fold Transforming growth factor, beta induced
2.0-fold Clade A, member 3G
2.0-fold Chemokine (C-C motif) ligand 2 (CCL2)
2.0-fold N-myc downstream regulated gene 1
2.0-fold Superoxide dismutase 2, mitochondrial
2.0-fold N-myc downstream regulated gene 1
2.0-fold ERBB receptor feedback inhibitor 1
2.0-fold 3-phosphoinositide dependent protein kinase-1

B.

C.

FIGURE 2. Tumor cell-mediated induction of mRNA and proteins in MC3T3-E1 cells with potential involvement in the up-regulation of MMP-13. *A,* Affymetrix microarray analysis of mRNAs showing increased expression (>2-fold) in MC3T3-E1 grown in the presence of MDA-1833 conditioned medium (*CM*) compared with base-level expression (*Base*). The heat map indicates the range of mRNA expression levels (*A*-values) and the fold changes in mRNA expression are indicated. All fold changes are significant with BH-adjusted p values < 0.05. MC3T3-E1 cells were treated with either serum-free or MDA-1833-conditioned media: *B,* quantitative real time PCR of MMP-13, MMP-2, OSMR, and gp130 mRNA levels. *C,* Western blotting of OSMR and gp130 protein with actin levels used as a comparative loading control.

multiple MMP-13-inducing factors in the conditioned media. However, a blocking antibody against the common gp130 IL-6 receptor partially inhibited the ability of the conditioned media to induce both STAT-3 phosphorylation and MMP-13 mRNA and protein expression (Fig. 3, *E* and *F*). Therefore, IL-6 family cytokines in the breast tumor cell/osteoblast co-culture microenvironment contribute to MMP-13 induction.

Proteomic Analysis of MC3T3-E1 Cells Using iTRAQ—Given the importance of MMP-13 in microenvironmental bone remodeling that could contribute to tumor cell colonization, we used a multiplex quantitative proteomic approach to investi-

gate the global effects of inducing MMP-13 expression in MC3T3-E1 cells by MDA-231 and MDA-1833 cells and to screen for potential MMP-13 substrates that may play a role in promoting breast cancer metastasis to bone. Differentiated MC3T3-E1 osteoblasts were cultured in the presence or absence of exogenous active MMP-13, and changes in the proteome profile of cells in the presence of MMP-13 were revealed using differential 2- or 4-plex iTRAQ labeling of the MC3T3-E1 cell culture supernatants and two-dimensional LC-MS/MS analysis. The data reported encompass three independent experiments, in which a total of 1280 proteins were identified
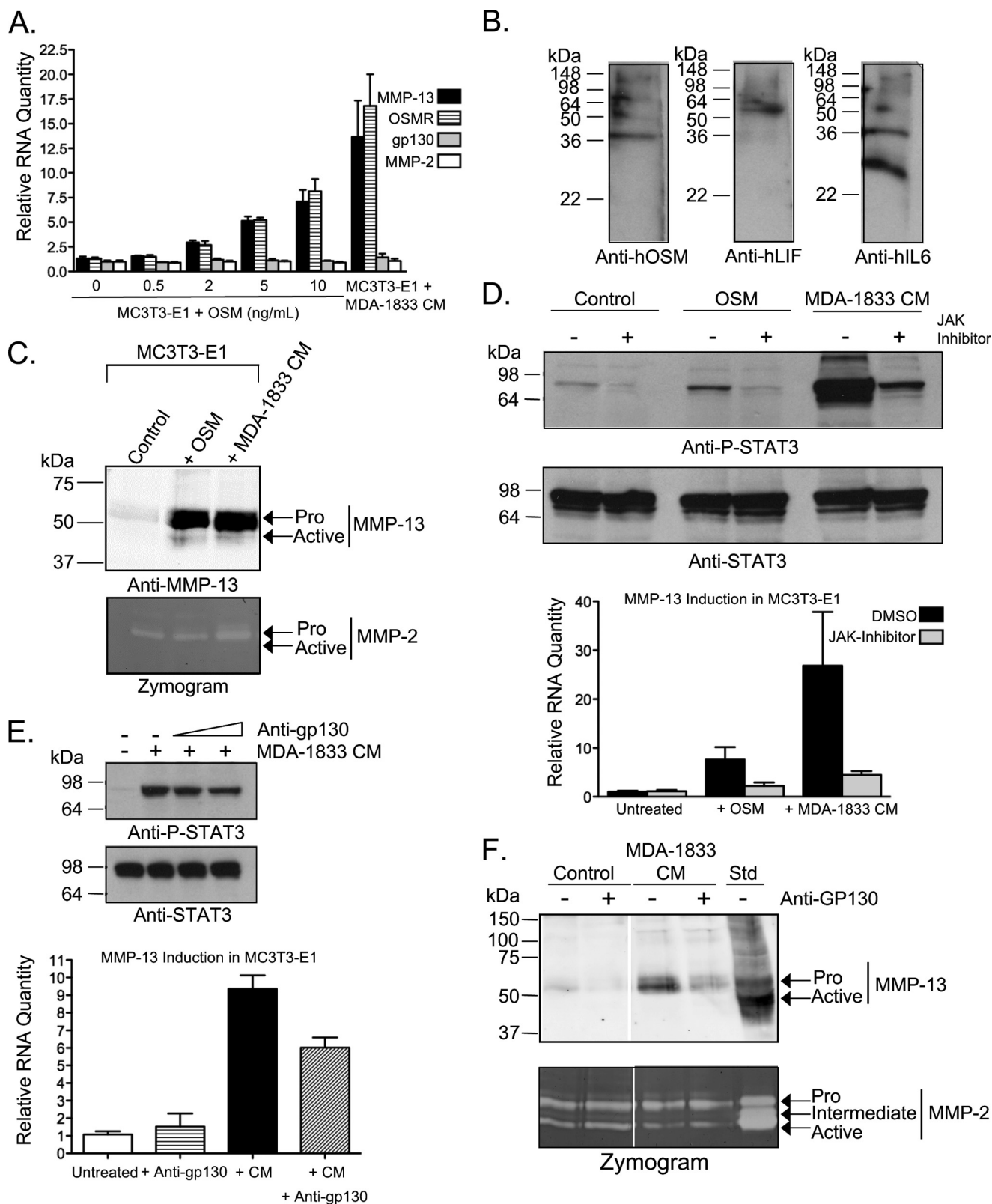
FIGURE 3. **MMP-13 induction by cytokines that induce STAT-3-dependent signaling.** *A,* QRT-PCR analysis of MMP-13, OSMR, gp130, and MMP-2 mRNA levels in MC3T3-E1 cells treated with the indicated dose of recombinant OSM or MDA-1833 cell-conditioned medium. *B,* Western blot analysis of OSM, LIF, and IL-6 expression in MDA-1833 cell-conditioned medium. MC3T3-E1 cells were incubated with 10 ng/ml OSM or MDA-1833 cell-conditioned medium and analyzed by Western blot for MMP-13 induction, with the zymogram of MMP-2 included as a control (*C*) and phospho-STAT-3 signaling in the absence or presence of a JAK-1 inhibitor with total STAT-3 as a loading control and analysis of MMP-13 mRNA induction by QRT-PCR in the presence of the inhibitor (*D*). MC3T3-E1 cells treated with MDA-1833 cell-conditioned medium in the absence or presence of a function-blocking antibody against the common gp130 subunit of the OSM, LIF, and IL-6 receptors. Phospho-STAT-3 signaling was assessed by Western blotting (*D*) and MMP-13 mRNA induction by QRT-PCR (*D*) and Western blotting (*E*), with the zymogram of MMP-2 included to show selectivity of the response to MMP-13. *CM,* cell-conditioned medium; *Std,* pro and active MMP-13 as standards.

TABLE 2

Proteomic iTRAQ analysis of MC3T3-E1 cells

Proteins that increased or decreased in the cell culture supernatants after incubation with MMP-13 are shown. Protein iTRAQ ratios are given as averages from three experiments with standard deviations from cultures treated with 0.1 and 1 μg/ml MMP-13 compared with untreated cells. Also, for each experiment the number of peptides used in the quantification of the protein, which may include peptides of the same sequence, are given, and the total number of unique peptides used in the identification of the protein are indicated in parentheses. NF indicates not found.

		Ratio MMP13:Control		Peptides		
Accession #	Protein Name	0.1 μg/mL	1 μg/mL	Exp 1	Exp 2	Exp 3
Proteins or proteolytic fragments that increased in cell culture supernatants treated with MMP-13						
IPI00136642.1	Antithrombin-III	2.9	2.5	NF	1 (4)	NF
IPI00117811.2	AP-3 complex subunit delta-1	1.5 ± 0.38	1.5 ± 0.17	NF	1 (2)	1 (2)
IPI00453793.4	AT-hook transcription factor	NF	15.3	1 (9)	NF	NF
IPI00399958.3	Calumenin isoform 2	2.3 ± 0.16	2.0 ± 0.46	NF	2 (10)	2 (11)
IPI00108087.1	CCL2 (MCP-1)	1.2	3.1	6 (10)	2 (2)	NF
IPI00131236.1	CCL7 (MCP-3)	1.7	1.7	NF	1 (1)	NF
IPI00153809.1	CD109 antigen homolog	1.3 ± 0.24	1.3 ± 0.15	NF	1 (3)	1 (4)
IPI00396802.1	Chromodomain helicase-DNA-binding protein 4	7.5	6.0	NF	1 (5)	NF
IPI00132473.3	Cleavage and polyadenylation specificity factor 5	2.0	1.9	NF	NF	1 (1)
IPI00409405.2	Cofilin-1	1.4 ± 0.13	1.4 ± 0.08	NF	1 (5)	1 (6)
IPI00775783.1	Complement component 1q	1.4	1.5	NF	NF	2 (2)
IPI00114065.1	Complement factor B	NF	4.1	3 (8)	NF	NF
IPI00133103.1	Creg1 Protein	1.3	1.5	NF	1 (32)	NF
IPI00459280.2	Dcps Scavenger mRNA-decapping enzyme	1.9	1.5	NF	NF	1 (4)
IPI00320241.1	DnaJ homolog subfamily B member 11	2.3	2.3	NF	NF	1 (3)
IPI00230415.5	Eukaryotic translation initiation factor 2 subunit 3	1.6	1.6	NF	1 (3)	NF
IPI00395038.2	Exportin-1	1.3 ± 0.60	1.5 ± 0.57	NF	1 (2)	2 (2)
IPI00112414.1	Exportin-2	1.4	1.5	NF	1 (3)	NF
IPI00648993.1	Growth factor receptor bound protein 2	1.5	1.3	NF	NF	2 (4)
IPI00111957.3	Histone H2B type 1-A	NF	2.9	2 (4)	NF	NF
IPI00173156.1	LZIC Protein	1.4 ± 0.10	1.3 ± 0.21	NF	4 (6)	3 (4)
IPI00788387.1	Milk fat globule-EGF factor 8 protein isoform 1	1.6 ± 0.03	1.7 ± 0.06	NF	1 (2)	1 (1)
IPI00320188.5	Nicotinamide phosphoribosyltransferase	0.9	1.8	NF	1 (2)	NF
IPI00127417.1	Nucleoside diphosphate kinase B	1.2 ± 0.05	1.5 ± 0.49	12 (14)	9 (10)	14 (11)
IPI00626467.1	Pcdhgc3 protein	1.7	NF	NF	NF	1 (1)
IPI00404438.1	Phosphatidylinositol-binding clathrin assembly protein 6	1.5 ± 0.51	1.6 ± 0.43	NF	4 (5)	3 (4)
IPI00755389.1	Phosphoribosyl pyrophosphate synthetase-assoc. protein 1	1.3	1.6	NF	NF	1 (3)
IPI00118819.1	Platelet-activating factor acetylhydrolase IB subunit γ	1.6	1.7	NF	NF	1 (1)
IPI00461914.1	Platelet-derived growth factor, C polypeptide	1.0 ± 0.11	1.3 ± 0.40	5 (7)	6 (6)	7 (7)
IPI00378557.2	Prefoldin subunit 4	1.4	1.5	NF	NF	3 (4)
IPI00816941.1	PRKC apoptosis WT1 regulator protein 2	2.0 ± 0.60	1.7 ± 0.85	NF	1 (3)	2 (3)
IPI00461933.2	Protein CutA Isoform 1	2.4 ± 0.45	1.5 ± 0.67	1 (3)	3 (2)	3 (3)
IPI00133985.1	RuvB-like 1	1.6	1.5	NF	1 (2)	NF
IPI00114945.1	Septin-2	1.6	1.4	NF	NF	3 (4)

TABLE 2—*continued*

IPI00224626.3	Septin-7	2.5	2.6	NF	NF	1 (4)
IPI00120760.1	Serum amyloid A-3 protein	NF	10.8	8 (4)	NF	NF
IPI00757958.1	SET-binding factor 2	NF	26.2	1 (11)	NF	NF
IPI00317966.5	Steroid receptor RNA activator 1	NF	4.1	1 (3)	NF	NF
IPI00816839.1	SUMO-activating enzyme subunit 1 Isoform 2	1.7	1.6	NF	NF	1 (1)
IPI00756257.1	Titin	NF	2.6	7 (148)	NF	NF
IPI00395051.2	Transmembrane protein 119	2.2	2.3	NF	NF	1 (1)
IPI00115498.1	Tumor necrosis factor receptor superfamily member 11B	1.8 ± 0.18	2.0 ± 0.34	NF	1 (3)	3 (6)
IPI00112506.2	Twisted gastrulation protein homolog 1	1.5	1.5	NF	3 (1)	NF
IPI00116552.1	Tyrosylprotein sulfotransferase 1	1.5 ± 0.23	1.3 ± 0.24	NF	3 (4)	4 (3)
IPI00123313.1	Ubiquitin-activating enzyme E1 X	1.4 ± 0.13	1.4 ± 0.17	NF	5 (6)	9 (10)
IPI00624876.2	Vasodilator-stimulated phosphoprotein	4.2 ± 4.43	5.2 ± 2.47	NF	2 (3)	1 (2)
Proteins or proteolytic fragments that decreased in cell culture supernatants treated with MMP-13						
IPI00126140.1	ADAM 12	NF	0.7	1 (3)	NF	NF
IPI00469188.3	ADAMTS-4	0.7 ± 0.08	0.7 ± 0.15	2 (7)	3 (3)	2 (2)
IPI00123063.5	CAP-Gly domain-containing linker protein 1	0.4	0.4	NF	2 (9)	NF
IPI00321647.2	Eukaryotic translation initiation factor 3 sub 8	0.5 ± 0.10	0.4 ± 0.06	NF	2 (2)	4 (5)
IPI00113223.2	Fatty acid synthase	0.7	0.6	1 (18)	NF	5 (11)
IPI00649913.1	LIM and SH3 protein 1	0.7 ± 0.02	0.7 ± 0.07	3 (7)	6 (4)	10 (9)
IPI00111960.2	Lysosomal alpha-glucosidase	0.7 ± 0.15	0.8 ± 0.11	1 (5)	8 (10)	9 (9)
IPI00757220.2	Neogenin isoform	0.5	0.7	NF	NF	1 (1)
IPI00311626.5	Nucleosome-binding protein 1	0.2	0.4	NF	1 (1)	NF
IPI00515360.7	Perlecan	0.6 ± 0.05	0.8 ± 0.19	3 (53)	4 (61)	7 (61)
IPI00828976.	Thymopoietin isoform ε	0.6 ± 0.29	0.7 ± 0.19	NF	13 (12)	3 (10)

(confidence >95%) in MC3T3-E1 culture supernatants as presented in supplemental Tables S4–S7. The analysis of peptide isotope ratios in experiments designed like this is now a well established approach to proteomically identify protease substrates in cell culture systems (46, 76, 77, 78).

A summary of proteins that showed consistent changes in level upon incubation of MC3T3-E1 cells with MMP-13 are given in Table 2, where iTRAQ ratios are expressed as cells treated with MMP-13/untreated control. Ratios of >1 represent an increase of the protein or cleaved protein fragments in the culture supernatants that could be due to induction of expression or processing by MMP-13 to release proteins or cleaved protein fragments from the cell surface or pericellular matrix, either directly or indirectly by MMP-13. Conversely, an iTRAQ of <1 indicates a decrease in a protein in the culture supernatant suggesting possible processing or degradation, and again these may either be direct or indirect effects. A ratio cutoff of >1.3 and <0.7 was applied to identify changes in the proteome, as well as candidate novel MMP-13 substrates that were validated biochemically. Similar ratios were obtained when either 0.1 or 1 µg/ml MMP-13 was added to cultures. The reproducibility of the experiments was further indicated by the iTRAQ ratios determined for human MMP-13 protein that was added exogenously to the cell cultures. In samples where 1 µg/ml MMP-13 had been added, iTRAQ ratios of 9.6, 8.0, and 14.8 were determined, whereas samples with 0.1 µg/ml MMP-13 added had ratios of 1.7 and 3.2.

Forty eight proteins were identified that were increased between 1.3- and 26-fold in culture supernatants containing MMP-13, including CCL-7 (monocyte chemoattractant protein-3) (1.7-fold increase), which is cleaved by MMP-13 (Fig. 5A). In addition, three other proteins were identified that were previously shown to be cleaved by other MMPs as follows: complement component 1q (C1q) by MMP-14 (57), antithrombin III by MMP-3 (58), and SAA3 by MMP-1 and MMP-3 (59), indicating that these too were high confidence MMP-13 substrates. Eleven proteins were identified with iTRAQ ratios <1 (ratios 0.8 to 0.2) that had between 1.3- and 5-fold reduction in levels compared with the untreated control. These included the known MMP-13 substrate perlecan, further validating the analysis.

Addition of MMP-13 was found to impact the levels of a functionally diverse range of proteins, a number of which have known association with promoting tumor growth, angiogenesis, and metastasis, *e.g.* milk fat globule-EGF factor 8 protein isoform 1 (60, 61) and vasodilator-stimulated phosphoprotein (62). Impor-
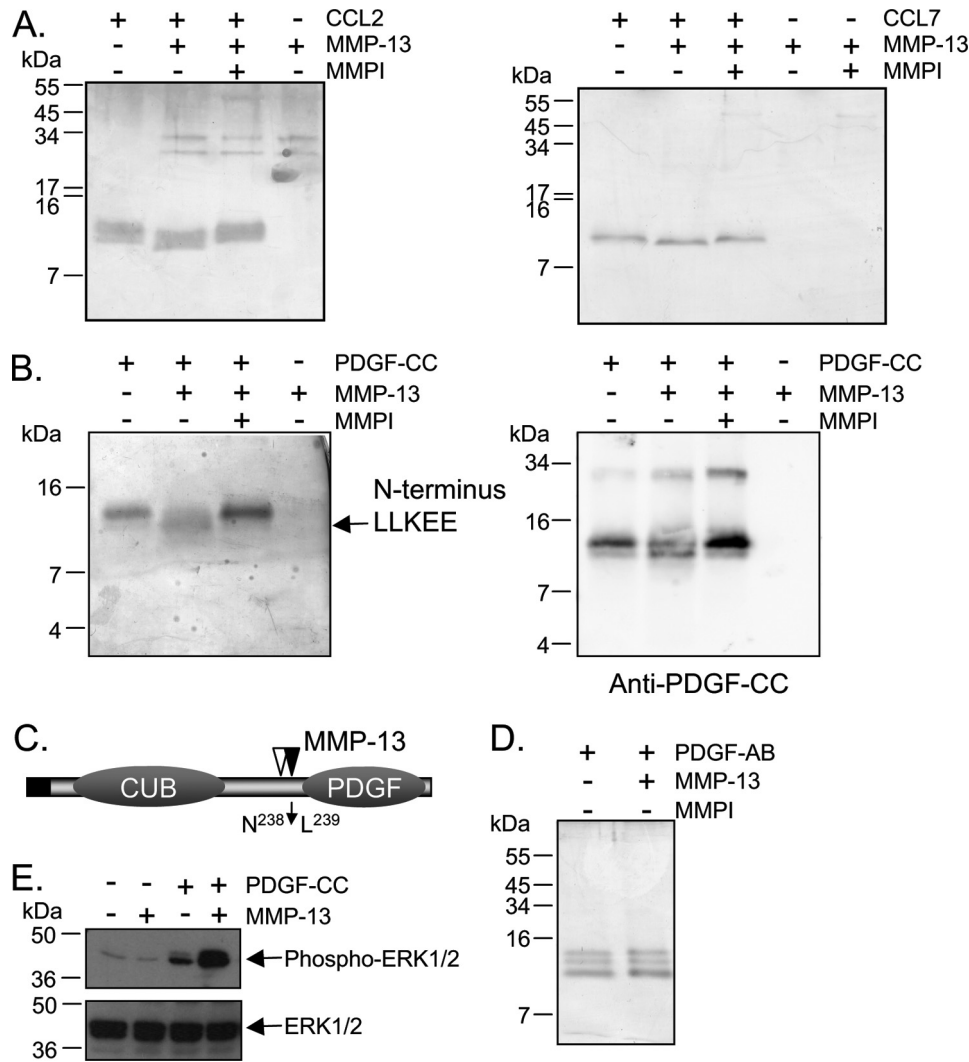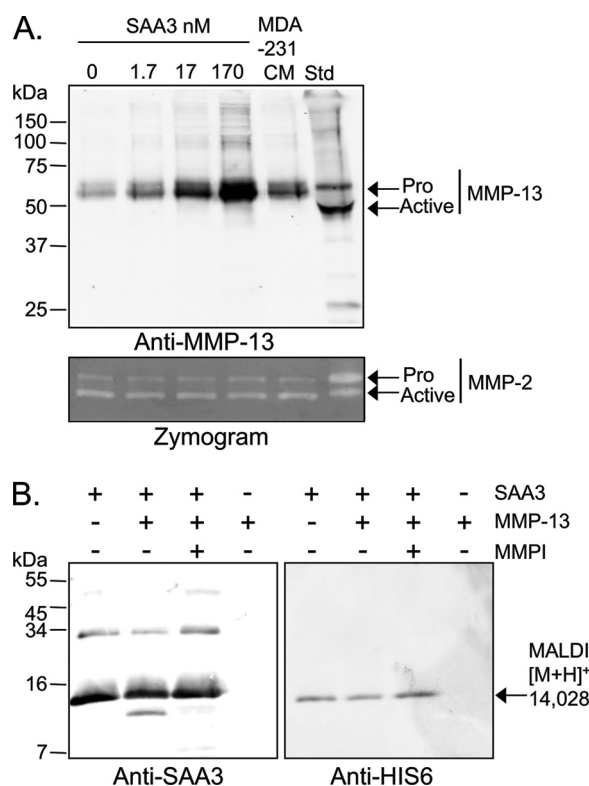
FIGURE 4. **Validation of MMP-13 substrates identified by iTRAQ proteomics analyses.** Substrates were incubated at 37 °C overnight alone or with active recombinant MMP-13 in the presence and absence of the MMP inhibitor (*MMPI*) marimastat. *A,* silver-stained Tris-Tricine SDS-PAGE of cleavage of chemokines CCL2 (MCP1) and CCL7 (MCP3). *B,* silver-stained Tris-Tricine SDS-PAGE and Western blot analysis of platelet-derived growth factor (PDGF)-CC analyzed under reducing conditions. The N terminus of the cleaved PDGF-C product as identified by Edman sequencing is given. *C,* schematic of the full-length PDGF-C monomer showing, from *left* to *right,* the signal sequence (*black domain*), inhibitory CUB, and bioactive PDGF domains. The cleavage sites are indicted for MMP-13 (*closed triangle*) and plasmin (*open triangle*). *D,* silver-stained Tris-Tricine SDS-PAGE of PDGF-AB cleavage assays analyzed under reducing conditions. *E,* Western blot analysis of phospho-ERK1/2 and total ERK1/2 in MC3T3 cells after the addition of recombinant PDGF-CC domain and PDGF-CC that had been cleaved by MMP-13.

tantly, many of the proteins elevated in MMP-13-treated cultures, *e.g.* chemokines CCL2 and CCL7, PDGF-C and SAA3 are known to recruit cells of the monocyte lineage, including osteoclasts, and to be important in osteoclast differentiation (63–67).
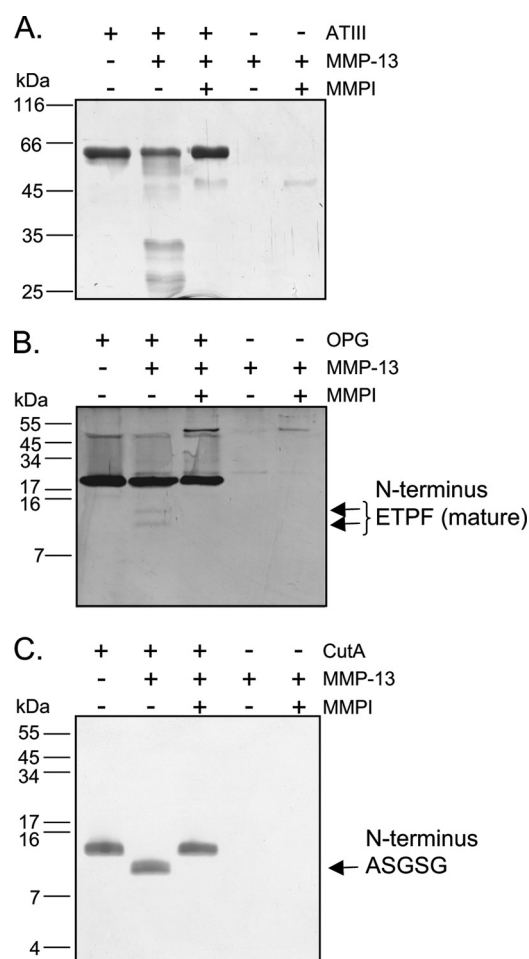
Validation of Candidate Substrates of MMP-13—To confirm that the proteins identified from high or low peptide ratios in these degradomics analyses were direct MMP-13 substrates, we performed secondary biochemical validation on six of the proteins that were found to be elevated in MC3T3-E1 culture supernatants after treatment with MMP-13. A 4-fold increase in CCL2 protein levels was observed in MC3T3-E1 culture supernatants incubated with MMP-13 (Table 2; supplemental Table S8), and Affymetrix microarray analysis of MC3T3-E1 cells incubated with MDA-1833-conditioned medium also revealed a 2-fold increase in CCL2 mRNA (BH-adjusted $p = 0.0001$) (Fig. 2*A*). Because a large number of chemokines are known substrates of MMPs (68), we postulated that CCL2 was

a likely, but not previously reported, MMP-13 substrate candidate. Indeed, MMP-13 efficiently cleaved CCL2 as shown by a small decrease in the molecular size of CCL2 on Tris-Tricine SDS-PAGE analysis that was blocked by the MMPI marimastat (Fig. 4*A*). A similar reduction in size was also seen when CCL7 was incubated with MMP-13 (Fig. 4*A*). The CCL2 cleavage product had a 384.3-Da reduction in mass as measured by MALDI-TOF MS consistent with the size difference expected following removal of the first five amino acids by cleavage between Ile-5 and Asn-6 and generation of an antagonist form of the chemokine as reported previously for cleavage by MMPs 1 and 3, which cleave at Ala-4 and Ile-5, and for CCL7 following MMP cleavage between Gly4 and Ile-5 (34). CCL2 and CCL7 cleavage by MMP-13 to generate antagonist forms may therefore represent a feedback mechanism in a monocyte recruitment pathway that appears to be controlled at least in part by MMP-13.

FIGURE 5. **Induction of MMP-13 expression by SAA3 in MC3T3-E1 cells and validation of SAA3 as a novel MMP-13 substrate.** *A,* Western blot analysis of MMP-13 induction in MC3T3-E1 cells incubated between 1.7 and 170 nM recombinant SAA3. Gelatin zymogram indicating MMP-2 expression is included as a control, and standards (*Std*) are purified recombinant MMP-13 or MMP-2. *B,* Western blot analysis using anti-SAA3 and anti-His$_6$ antibodies of MMP-13-cleaved recombinant SAA3. SAA3 was incubated at 37 °C overnight alone or with active recombinant MMP-13 in the presence and absence of the MMPI marimastat.

FIGURE 6. **Validation of MMP-13 substrates identified by iTRAQ proteomics analysis.** Substrates are incubated at 37 °C overnight, alone, or with active recombinant MMP-13 in the presence and absence of the MMPI marimastat. Silver-stained SDS-PAGE of antithrombin (*AT*) III (*A*), OPG (*B*), and protein CutA cleavage assays (*C*). Where determined, the N terminus of the cleaved products as identified by Edman sequencing is given.

PDGF-C is secreted in a latent homodimeric form that requires proteolytic processing of the N-terminal CUB domains to release the PDGF-CC growth factor domain that can bind and activate the PDGF-α receptor. A 1.3-fold increase in PDGF-C was observed in culture supernatants of osteoblasts incubated with 1 μg/ml MMP-13 (Table 2; supplemental Table S9). MMP-13 cleaved a recombinant form of PDGF-CC consisting of 15 amino acids of the linker domain after the putative plasmin/tissue plasminogen activator cleavage site and the PDGF domain. Tris-Tricine SDS-PAGE and Western blot analysis (Fig. 4*B*) detected a small decrease in the molecular size of the recombinant PDGF-CC incubated with MMP-13 compared with untreated PDGF-CC or PDGF-CC incubated with MMP-13 in the presence of marimastat. N-terminal sequencing confirmed that MMP-13 cleaved within the linker to generate a neo-N terminus starting with LLKEE leaving the PDGF domain intact (Fig. 4*C*). In contrast, MMP-13 did not cleave PDGF-AB (Fig. 4*D*), and indeed iTRAQ analysis of co-cultures indicated no change in PDGF-A levels, and PDGF-B was not detected (supplemental Table S4). The ability of the PDGF-CC to bind and activate the PDGF-α receptor expressed in MC3T3-E1 cells was investigated. An enhancement in the phosphorylation of ERK1/2, a signaling molecule downstream of PDGFR, was observed with MMP-13-cleaved PDGF-CC, compared with the uncleaved control (Fig. 4*E*).

A greater than 10-fold increase in the acute response phase apolipoprotein SAA3 was observed in MC3T3-E1 osteoblast culture supernatants after incubation with MMP-13 (Table 2; supplemental Table S10). We also demonstrated by Affymetrix analysis paracrine induction (4-fold increase BH-adjusted $p = 0.003$) of MC3T3-E1 SAA3 mRNA expression by MDA-1833-conditioned medium (Fig. 2*A*). To investigate the role of SAA3, we expressed an N-terminal His-tagged recombinant form of the protein in *E. coli* and purified the protein to homogeneity using a Ni^{2+}-chelate column. Notably, SAA3 was found to specifically induce MMP-13 protein expression in differentiated MC3T3-E1 osteoblasts at concentrations as low as 1.7 nM, with specificity indicated since MMP-2 expression remained unchanged (Fig. 5*A*). Interestingly, SAA3 was cleaved by MMP-13 with Western blot analysis using anti-SAA3 and anti-His antibodies revealing the removal of the N terminus of the protein (Fig. 5*B*). The size of the cleavage product generated by MMP-13 indicated that cleavage occurred at a unique site compared with MMP-1 and -3, which both generate a 6-kDa fragment that retains the original N terminus of the mature protein (69). Because cleavage of the SAA3 protein preparation was not

100% complete, we could not determine whether the cleaved product lost MMP-13-inductive properties.

The serine proteinase inhibitor antithrombin III increased ~2.7-fold after incubation of the cells with MMP-13. MMP-13 also efficiently cleaved antithrombin III-generating multiple fragments (Fig. 6A), including an ~10-kDa fragment with a neo-N terminus starting at amino acid position 243 (LTALV). The pattern observed for antithrombin III cleavage by MMP-13 differs from that reported for MMP-3, which cleaves only once within the reactive site loop of antithrombin III (58). Notably, this single cleavage results in loss of inhibitory activity. Interestingly, increased degradation of antithrombin III has been reported in both early and late stages of breast cancer, but the proteases involved were not identified.

TNF receptor superfamily member 11b or osteoprotegerin is the soluble decoy receptor for RANKL, which prevents excessive osteoclastogenesis and osteolysis. Osteoprotegerin was identified by six peptides and quantified by three peptides from the C terminus of the proteins that were all elevated ~2-fold in MC3T3-E1 supernatants following treatment with MMP-13 (Table 2; supplemental Table S11). MMP-13 cleaved recombinant osteoprotegerin, giving rise to two cleavage products, both of which retained the mature N terminus of the protein, suggesting that C-terminal truncation was occurring (Fig. 6B).

Protein CutA accumulated 2–3-fold in MMP-13-treated MC3T3-E1 cell supernatants in experiments two and three. A recombinant full-length form of rat CutA isoform 1 was cleaved by MMP-13 (Fig. 6C) with 34 amino acids being removed from the mature N terminus to generate a neo-N terminus commencing with ASGSGY, as determined by Edman sequencing. The function of protein CutA in mammals is unclear; however, it has been shown to have both intracellular and extracellular locations (70, 71).

DISCUSSION

We have demonstrated the influence that breast cancer cells can exert on stroma to alter the proteolytic potential within the tumor microenvironment. Co-culture of breast cancer and MC3T3-E1 osteoblast-like cells in a two-dimensional system resulted in perturbations in the signaling networks causing significant alterations in many bioactive molecules. One such change, the elevation of MMP-13 expression in the osteoblasts, is initiated by soluble factors, including IL-6 family cytokines that are produced by the breast tumor cells and osteoblasts. A microenvironmental amplifying loop was initiated by the breast cancer cells through the up-regulation of one receptor OSMR in the osteoblasts. Once up-regulated, MMP-13 can potentially further impact breast cancer metastasis to bone through cleavage of a number of bioactive proteins, and indeed six novel substrates were proteomically identified and biochemically confirmed. Notably, MMP-13 induced the acute phase response of apolipoprotein SAA3 in the osteoblastic MC3T3-E1 cells, which in turn increased MMP-13 expression to further reinforce the microenvironmental amplifying feedback loop. MMP-13 also can be involved in regulating osteoclast recruitment activity by cleavage of CCL2, CCL7, PDGF-C, and osteoprotegerin, the decoy receptor for RANKL, therefore increasing cellular activity and osteolysis. Hence, breast cancer cells metastasizing to bone amplify carcinogenic potential by the modulation of osteoblast gene expression and protease induction and subsequent post-translational control of numerous signaling pathways.

Using targeted microarrays, such as the human and murine versions of the CLIP-CHIP, has the advantage of identifying the complete protease and inhibitor profile of cells. Perhaps not surprisingly, because MDA-1833 are highly invasive cell lines with up-regulated expression of many proteases, we saw only minimal changes in the proteolytic profile of the tumor cells upon co-culture with the osteoblasts (supplemental Table S1). The osteoblasts, however, when co-cultured with MDA-1833 cells exhibited several significant changes in their proteolytic profile. We focused on MMP-13, which showed the greatest change, increasing 6-fold, and has *in vivo* relevance as many studies have demonstrated a correlation between breast cancer progression and MMP-13 expression (72–74). MMP-13 mRNA has been shown to be elevated in tumor cells at the tumor-bone interface in a syngeneic mouse model where tumor cells were injected into the calvaria of BALB/c mice (75). In addition, in xenograft mouse models of breast cancer using MDA-231 cells, MMP-13 along with its potential activator MMP-14 were shown to be elevated in the stroma of xenografts in mammary fat pads and in bone. However, the cellular origin of MMP-13 was unclear, and the means of induction, as well as the effects of elevated expression of MMP-13, were not addressed (20). This pointed to the need for studies to clarify the tumor-mediated induction pathways for MMP-13 in osteoblasts and to identify the relevant substrates and hence the *in vivo* roles of MMP-13 that impact metastatic potential.

Analysis of our Affymetrix expression data suggested that the OSM pathway was activated in osteoblasts after they were treated with tumor cell-conditioned medium. We confirmed that the OSMR receptor subunit was elevated and that the cognate gp130/IL-6 cytokine receptor subunit was present. In addition, we showed that the tumor cells expressed OSM and that recombinant OSM treatment induced MMP-13 expression in the osteoblasts. The latter result was not surprising given that IL-6 family cytokines are known to activate STAT-3 translocation to the nucleus where it binds to and activates the MMP-13 promoter in chondrocytic cells (55). Clearly, JAK/STAT signaling is critical to this activation in osteoblasts. As well, we found that a pharmacological inhibition of the pathway very efficiently blocked MMP-13 induction by both recombinant OSM and tumor cell-conditioned medium. However, it is important to point out that other IL-6 ligands were present in the conditioned medium, and we found that IL-6 was also up-regulated in the treated osteoblasts. These observations, and our finding that a separate induction of MMP-13 expression occurs through the up-regulation of SAA3, strongly suggest that multiple pathways feed into this MMP-13 microenvironmental amplification loop.

Proteomic screens are powerful techniques for comprehensively dissecting the perturbations that proteases exert on a proteome in a nonbiased manner, a field that has come to be known as degradomics. We pioneered the use of proteomic screens involving differential labeling such as iTRAQ and ICAT

to successfully identify novel MMP-2 (76, 77) and MMP-14 (78, 79) substrates. The effects of tumor-induced elevated MMP-13 expression in osteoblasts on a proteome-wide scale have not been previously reported. Of the 1280 osteoblast proteins identified, 57 proteins were found to show consistent changes in expression in MMP-13-treated cells. By understanding the roles of these candidate substrates, the biological role for MMP-13 can be deciphered and hypotheses generated for testing in future studies.

Proteases such as the MMPs are key nodes in the protease web, a network whereby individual protease do not function alone but form cascades and regulatory circuits that are dynamically interconnected (7). We identified many changes in the protease and inhibitor profile of co-cultured (Table 1; Fig. 2A) or MMP-13-treated osteoblasts (Table 2), at the mRNA or proteome level, respectively. Our proteomic data demonstrate the "knock-on" effects that inducing or elevating expression of one protease can have. For example, upon incubating osteoblasts with MMP-13, we saw a reduction in two metalloproteinases ADAM-12 and ADAMTS-4 that could impact downstream substrates and pathways. In addition, the potent serine proteinase inhibitor antithrombin III, a major regulator of the coagulation cascade, was increased 2–3-fold in culture supernatants perhaps through release from binding to glycosaminoglycans in the extracellular matrix (80). However, antithrombin III was also processed by cleavages that are predicted to inactivate the inhibitor, thus potentially increasing the activity levels of many serine proteases, including thrombin. In the tumor microenvironment, this could ultimately impact expression levels of many MMPs, including MMP-2, -9, -10, -13, and -14, which are induced by thrombin interaction with the protease-activated receptor-1 (81–85). Two other proteins that can induce MMP expression were increased in culture supernatants, SAA3 and PDGF-C. SAA3 induces MMP-13 in MC3T3-E1 cells (Fig. 5A) and PDGF-C induces MMP-9 expression in monocytes (65). Although PDGFRα activation has been implicated in mechanical strain induction of MMP-13 in MC3T3-E1 cells (86), PDGF-CC, which activates PDGFRα, did not induce MMP-13 in these cells (data not shown). More directly, perturbation of the protease web can occur through the ability of MMP-13 to activate MMP-9 (87) and thus potentially further modulate the proteolytic activity of the tumor cells, which express MMP-9. MMP-13 produced by osteoblasts has been implicated in promoting osteoclast recruitment and osteolysis through the activation of MMP-9 (75). Further proteomic experiments are required to address the effects of osteoblastic MMP-13 expression on tumor cells and osteoclasts.

The defective skeletal growth plate development phenotype described for *Mmp13*-null mice was accompanied by a delay in osteoclast migration and recruitment (21). Interestingly, a number of the proteins that showed elevated expression in the presence of MMP-13, perhaps due to release of these proteins from the matrix, for example CCL2 and CCL7, SAA3, and PDGFs, are known to be involved in monocyte and osteoclast recruitment (34, 63–67). Our Affymetrix data indicated that tumor cells could also influence the expression of CCL2 in osteoblasts, as well as CXCL12 (SDF-1) (Fig. 2A). CC chemokines such as CCL2 and CCL7 are inflammatory mediators that

play pleiotropic tumorigenic roles in breast cancer homing to bone and metastases growth, through osteoblast induction, osteoclast resorption, and bone remodeling (88) with knockdown of CCL2 expression in MDA-231 cells reducing *in vivo* metastasis (89). In addition, a recent study demonstrated that CCL2 expressed by both metastatic breast cancer tumors and stroma plays a critical role in tumor cell extravasation and metastatic seeding that is mediated via inflammatory monocyte recruitment (90). We showed that cleavage of CCL2 and CCL7 by MMP-13 (Fig. 4A) generates forms of the chemokines that are potent receptor antagonists (34, 45) and so perhaps are part of a feedback mechanism.

In a lung metastasis model, primary tumor induction of SAA3 expression in pre-metastatic lungs resulted in recruitment of myeloid cells and accelerated migration of primary tumor cells to the lungs (66). SAA3 therefore has the potential to play a similar role in facilitating breast cancer tumor metastasis to bone. MMP-13 and SAA3 expression appeared to be integrally linked because SAA3 protein was increased 10-fold in osteoblast culture supernatant after incubation with MMP-13, and SAA3 specifically induced MMP-13 expression in the cells. Also, tumor cells mediated a 3.7-fold increase in MC3T3-E1 SAA3 expression. We also showed that MMP-13 cleaved SAA3 at the N terminus, and again this might be part of a feedback mechanism. When PDGF-CC is activated by removal of the inhibitory CUB domains, the PDGF-CC domain can then bind to its receptor PDGFRα and through autocrine or paracrine signaling can stimulate tumor growth and angiogenesis. The CUB domains are also involved in binding to the extracellular matrix (91). Because PDGF proteins are deposited in the bone matrix by osteoblasts and released by osteolysis (92, 93), MMP-13 cleavage of PDGF-CC in the hinge region could be involved in release of the active domain. Indeed, recombinant PDGF-CC domain cleaved by MMP-13 within the linker caused enhanced ERK1/2 phosphorylation compared with the control, which is a recombinant analogue of the plasmin-activated PDGF-CC, when added to MC3T3-E1 cells (Fig. 4E).

We also chose to investigate MMP-13 processing of CutA, a protein that has no known function in cancer. In *E. coli* CutA is involved in copper tolerance (94), and in humans CutA is required for the localization of acetylcholinesterase at the cell surface in brain (95–97). It has been postulated that CutA plays a role in signal transduction (98) and is one of 35 genes responsible for lactation (99), so the physiological role of CutA remains unclear. CutA may have dual roles, because it has been shown to be expressed in the cytoplasm and to undergo unconventional secretion, and so is a "moonlighting" protein (100). CutA was increased in the supernatants of MMP-13-treated osteoblasts and was efficiently cleaved by MMP-13 at the N terminus, and further investigation will be required to determine the role of CutA in breast cancer.

Bone metastatic disease in breast cancer is predominantly osteolytic. MMPs are modulators of osteolysis and the vicious cycle, primarily through mobilization and activation of growth factors such as TGF-β. In addition, in prostate cancer MMP-7 promotes osteoclast activation through the release of soluble RANKL from osteoblasts (101). Osteolysis is controlled by a

balance in osteoblast expression of RANKL and the soluble decoy receptor for RANKL, OPG. Binding of RANKL to osteoprotegerin prevents binding to the RANK receptor on osteoclasts. Homodimers of OPG have a much higher binding affinity for RANKL, compared with the monomer. Dimerization occurs by the death domains of OPG and also in part through interaction in the C-terminal heparin-binding region (102). Here, we show a 2-fold increase in osteoprotegerin levels in the presence of MMP-13, potentially through the release of heparin-bound OPG, which might be expected to lead to an overall reduction in osteolysis. However, because cleavage of OPG by MMP-13 results in C-terminal truncation, this might profoundly affect OPG activity.

Hence, our study has revealed the influence that tumors exert on the bone microenvironment through manipulation of signaling pathways in the osteoblast, which result in alteration of the balance of the protease repertoire. The subsequent impact that such modulation has is evident from the large catalogue of changes to the osteoblast proteome identified by our proteomics analysis. The ultimate outcome is a new molecular viscous cycle, whereby the breast cancer metastases secrete factors that induce osteoblasts to produce MMP-13. MMP-13 in turn activates these inducers, further stimulating MMP-13 expression, which then sculpts the metastases microenvironment.

REFERENCES

1. Nagaraja, G. M., Othman, M., Fox, B. P., Alsaber, R., Pellegrino, C. M., Zeng, Y., Khanna, R., Tamburini, P., Swaroop, A., and Kandpal, R. P. (2006) *Oncogene* **25,** 2328–2338
2. Minn, A. J., Gupta, G. P., Siegel, P. M., Bos, P. D., Shu, W., Giri, D. D., Viale, A., Olshen, A. B., Gerald, W. L., and Massagué, J. (2005) *Nature* **436,** 518–524
3. Gupta, G. P., Nguyen, D. X., Chiang, A. C., Bos, P. D., Kim, J. Y., Nadal, C., Gomis, R. R., Manova-Todorova, K., and Massagué, J. (2007) *Nature* **446,** 765–770
4. Kang, Y., Siegel, P. M., Shu, W., Drobnjak, M., Kakonen, S. M., Cordón-Cardo, C., Guise, T. A., and Massagué, J. (2003) *Cancer Cell* **3,** 537–549
5. Schwarz, E. M., and Ritchlin, C. T. (2007) *Arthritis Res. Ther.* **9,** Suppl. 1, 7
6. Terpos, E., Efstathiou, E., Christoulas, D., Roussou, M., Katodritou, E., and Dimopoulos, M. A. (2009) *Expert Opin. Biol. Ther.* **9,** 465–479
7. Overall, C. M., and Kleifeld, O. (2006) *Nat. Rev. Cancer* **6,** 227–239
8. Egeblad, M., and Werb, Z. (2002) *Nat. Rev. Cancer* **2,** 161–174
9. Chabottaux, V., and Noel, A. (2007) *Clin. Exp. Metastasis* **24,** 647–656
10. Lee, J., Weber, M., Mejia, S., Bone, E., Watson, P., and Orr, W. (2001) *Eur. J. Cancer* **37,** 106–113
11. Balbín, M., Fueyo, A., Tester, A. M., Pendás, A. M., Pitiot, A. S., Astudillo, A., Overall, C. M., Shapiro, S. D., and López-Otín, C. (2003) *Nat. Genet.* **35,** 252–257
12. Szabova, L., Chrysovergis, K., Yamada, S. S., and Holmbeck, K. (2008) *Oncogene* **27,** 3274–3281
13. Andarawewa, K. L., Boulay, A., Masson, R., Mathelin, C., Stoll, I., Tomasetto, C., Chenard, M. P., Gintz, M., Bellocq, J. P., and Rio, M. C. (2003) *Cancer Res.* **63,** 5844–5849
14. Jost, M., Folgueras, A. R., Frérart, F., Pendas, A. M., Blacher, S., Houard, X., Berndt, S., Munaut, C., Cataldo, D., Alvarez, J., Melen-Lamalle, L., Foidart, J. M., López-Otín, C., and Noël, A. (2006) *Cancer Res.* **66,** 5234–5241
15. Pendás, A. M., Folgueras, A. R., Llano, E., Caterina, J., Frerard, F., Rodrí-guez, F., Astudillo, A., Noël, A., Birkedal-Hansen, H., and López-Otín, C.
16. Overall, C. M., and Blobel, C. P. (2007) *Nat. Rev. Mol. Cell Biol.* **8,** 245–257
17. Freije, J. M., Díez-Itza, I., Balbín, M., Sánchez, L. M., Blasco, R., Tolivia, J., and López-Otín, C. (1994) *J. Biol. Chem.* **269,** 16766–16773
18. Acuff, H. B., Carter, K. J., Fingleton, B., Gorden, D. L., and Matrisian, L. M. (2006) *Cancer Res.* **66,** 259–266
19. Zigrino, P., Kuhn, I., Bäuerle, T., Zamek, J., Fox, J. W., Neumann, S., Licht, A., Schorpp-Kistner, M., Angel, P., and Mauch, C. (2009) *J. Invest. Dermatol.* **129,** 2686–2693
20. Lafleur, M. A., Drew, A. F., de Sousa, E. L., Blick, T., Bills, M., Walker, E. C., Williams, E. D., Waltham, M., and Thompson, E. W. (2005) *Int. J. Cancer* **114,** 544–554
21. Inada, M., Wang, Y., Byrne, M. H., Rahman, M. U., Miyaura, C., López-Otín, C., and Krane, S. M. (2004) *Proc. Natl. Acad. Sci. U.S.A.* **101,** 17192–17197
22. Stickens, D., Behonick, D. J., Ortega, N., Heyer, B., Hartenstein, B., Yu, Y., Fosang, A. J., Schorpp-Kistner, M., Angel, P., and Werb, Z. (2004) *Development* **131,** 5883–5895
23. Franchimont, N., Rydziel, S., Delany, A. M., and Canalis, E. (1997) *J. Biol. Chem.* **272,** 12144–12150
24. Uría, J. A., Jiménez, M. G., Balbín, M., Freije, J. M., and López-Otín, C. (1998) *J. Biol. Chem.* **273,** 9769–9777
25. Kusano, K., Miyaura, C., Inada, M., Tamura, T., Ito, A., Nagase, H., Kamoi, K., and Suda, T. (1998) *Endocrinology* **139,** 1338–1345
26. Varghese, S., Yu, K., and Canalis, E. (1999) *Am. J. Physiol.* **276,** E465–E471
27. Selvamurugan, N., Brown, R. J., and Partridge, N. C. (2000) *J. Cell. Biochem.* **79,** 182–190
28. Knäuper, V., Will, H., López-Otin, C., Smith, B., Atkinson, S. J., Stanton, H., Hembry, R. M., and Murphy, G. (1996) *J. Biol. Chem.* **271,** 17124–17131
29. Fosang, A. J., Last, K., Knäuper, V., Murphy, G., and Neame, P. J. (1996) *FEBS Lett.* **380,** 17–20
30. Knäuper, V., Cowell, S., Smith, B., López-Otin, C., O'Shea, M., Morris, H., Zardi, L., and Murphy, G. (1997) *J. Biol. Chem.* **272,** 7608–7616
31. Monfort, J., Garcia-Giralt, N., López-Armada, M. J., Monllau, J. C., Bonilla, A., Benito, P., and Blanco, F. J. (2006) *Arthritis Res. Ther.* **8,** R149
32. Monfort, J., Tardif, G., Roughley, P., Reboul, P., Boileau, C., Bishop, P. N., Pelletier, J. P., and Martel-Pelletier, J. (2008) *Osteoarthritis Cartilage* **16,** 749–755
33. McQuibban, G. A., Butler, G. S., Gong, J. H., Bendall, L., Power, C., Clark-Lewis, I., and Overall, C. M. (2001) *J. Biol. Chem.* **276,** 43503–43508
34. McQuibban, G. A., Gong, J. H., Wong, J. P., Wallace, J. L., Clark-Lewis, I., and Overall, C. M. (2002) *Blood* **100,** 1160–1167
35. Tarín, C., Gomez, M., Calvo, E., López, J. A., and Zaragoza, C. (2009) *Arterioscler. Thromb. Vasc. Biol.* **29,** 27–32
36. Hashimoto, G., Inoki, I., Fujii, Y., Aoki, T., Ikeda, E., and Okada, Y. (2002) *J. Biol. Chem.* **277,** 36288–36295
37. Dangelo, M., Sarment, D. P., Billings, P. C., and Pacifici, M. (2001) *J. Bone Miner. Res.* **16,** 2339–2347
38. Kahai, S., Vary, C. P., Gao, Y., and Seth, A. (2004) *Matrix Biol.* **23,** 445–455
39. Overall, C. M., and Sodek, J. (1990) *J. Biol. Chem.* **265,** 21141–21151
40. Kappelhoff, R., and Overall, C. (2009) *Current Protocols Protein Science*, Supplement 49, **Unit 21.19,** 1–16
41. Kappelhoff, R., auf dem Keller, U., and Overall., C. M. (2010) in *Methods in Molecular Biology* (Clarke, I. M., ed) pp. 175–193, Springer-Verlag Inc., New York
42. Butler, G. S., Tam, E. M., and Overall, C. M. (2004) *J. Biol. Chem.* **279,** 15615–15620
43. Morrison, C. J., Butler, G. S., Bigg, H. F., Roberts, C. R., Soloway, P. D., and Overall, C. M. (2001) *J. Biol. Chem.* **276,** 47402–47410
44. Lin, Y., Rajala, M. W., Berger, J. P., Moller, D. E., Barzilai, N., and Scherer, P. E. (2001) *J. Biol. Chem.* **276,** 42077–42083
45. McQuibban, G. A., Gong, J. H., Tam, E. M., McCulloch, C. A., Clark-Lewis, I., and Overall, C. M. (2000) *Science* **289,** 1202–1206

46. Butler, G. S., Dean, R. A., Morrison, C. J., and Overall, C. M. (2010) in *Methods in Molecular Biology* (Clarke, I. M., ed) pp. 451–470, Springer-Verlag Inc., New York

47. auf dem Keller, U., Bellac, C. L., Li, Y., Lou, Y., Lange, P. F., Ting, R., Harwig, C., Kappelhoff, R., Dedhar, S., Adam, M. J., Ruth, T. J., Bénard, F., Perrin, D. M., and Overall, C. M. (2010) *Cancer Res.* **70,** 7562–7569

48. Zhang, J., Shridhar, R., Dai, Q., Song, J., Barlow, S. C., Yin, L., Sloane, B. F., Miller, F. R., Meschonat, C., Li, B. D., Abreo, F., and Keppler, D. (2004) *Cancer Res.* **64,** 6957–6964

49. Ozaki, N., Ohmuraya, M., Hirota, M., Ida, S., Wang, J., Takamori, H., Higashiyama, S., Baba, H., and Yamamura, K. (2009) *Mol. Cancer Res.* **7,** 1572–1581

50. Cowell, S., Knäuper, V., Stewart, M. L., D'Ortho, M. P., Stanton, H., Hembry, R. M., López-Otín, C., Reynolds, J. J., and Murphy, G. (1998) *Biochem. J.* **331,** 453–458

51. Filanti, C., Dickson, G. R., Di Martino, D., Ulivi, V., Sanguineti, C., Romano, P., Palermo, C., and Manduca, P. (2000) *J. Bone Miner. Res.* **15,** 2154–2168

52. Mizutani, A., Sugiyama, I., Kuno, E., Matsunaga, S., and Tsukagoshi, N. (2001) *J. Bone Miner. Res.* **16,** 2043–2049

53. Nakano, Y., Forsprecher, J., and Kaartinen, M. T. (2010) *J. Cell. Physiol.* **223,** 260–269

54. Bisson, C., Blacher, S., Polette, M., Blanc, J. F., Kebers, F., Desreux, J., Tetu, B., Rosenbaum, J., Foidart, J. M., Birembaut, P., and Noel, A. (2003) *Int. J. Cancer* **105,** 7–13

55. Heinrich, P. C., Behrmann, I., Haan, S., Hermanns, H. M., Müller-Newen, G., and Schaper, F. (2003) *Biochem. J.* **374,** 1–20

56. El Mabrouk, M., Sylvester, J., and Zafarullah, M. (2007) *Biochim. Biophys. Acta* **1773,** 309–320

57. Rozanov, D. V., Ghebrehiwet, B., Postnova, T. I., Eichinger, A., Deryugina, E. I., and Strongin, A. Y. (2002) *J. Biol. Chem.* **277,** 9318–9325

58. Mast, A. E., Enghild, J. J., Nagase, H., Suzuki, K., Pizzo, S. V., and Salvesen, G. (1991) *J. Biol. Chem.* **266,** 15810–15816

59. Vallon, R., Freuler, F., Desta-Tsedu, N., Robeva, A., Dawson, J., Wenner, P., Engelhardt, P., Boes, L., Schnyder, J., Tschopp, C., Urfer, R., and Baumann, G. (2001) *J. Immunol.* **166,** 2801–2807

60. Neutzner, M., Lopez, T., Feng, X., Bergmann-Leitner, E. S., Leitner, W. W., and Udey, M. C. (2007) *Cancer Res.* **67,** 6777–6785

61. Jinushi, M., Nakazaki, Y., Carrasco, D. R., Draganov, D., Souders, N., Johnson, M., Mihm, M. C., and Dranoff, G. (2008) *Cancer Res.* **68,** 8889–8898

62. Han, G., Fan, B., Zhang, Y., Zhou, X., Wang, Y., Dong, H., Wei, Y., Sun, S., Hu, M., Zhang, J., and Wei, L. (2008) *Oncol. Rep.* **20,** 929–939

63. Yu, X., Huang, Y., Collin-Osdoby, P., and Osdoby, P. (2004) *J. Bone Miner. Res.* **19,** 2065–2077

64. Han, C. Y., Subramanian, S., Chan, C. K., Omer, M., Chiba, T., Wight, T. N., and Chait, A. (2007) *Diabetes* **56,** 2260–2273

65. Wågsäter, D., Zhu, C., Björck, H. M., and Eriksson, P. (2009) *Atherosclerosis* **202,** 415–423

66. Hiratsuka, S., Watanabe, A., Sakurai, Y., Akashi-Takamura, S., Ishibashi, S., Miyake, K., Shibuya, M., Akira, S., Aburatani, H., and Maru, Y. (2008) *Nat. Cell Biol.* **10,** 1349–1355

67. Soria, G., and Ben-Baruch, A. (2008) *Cancer Lett.* **267,** 271–285

68. Cox, J. H., and Overall, C. M. (2008) in *The Cancer Degradome: Proteases and Cancer Biology* (Edwards, D., Hoyer-Hansen, G., Blasi, F., and Sloan, B. F., eds) pp. 519–540, Springer-Verlag Inc., New York

69. Mitchell, T. I., Jeffrey, J. J., Palmiter, R. D., and Brinckerhoff, C. E. (1993) *Biochim. Biophys. Acta* **1156,** 245–254

70. Liang, D., Carvalho, S., Bon, S., and Massoulié, J. (2009) *FEBS J.* **276,** 4473–4482

71. Liang, D., Nunes-Tavares, N., Xie, H. Q., Carvalho, S., Bon, S., and Massoulié, J. (2009) *J. Biol. Chem.* **284,** 5195–5207

72. Pendás, A. M., Uría, J. A., Jiménez, M. G., Balbín, M., Freije, J. P., and López-Otín, C. (2000) *Clin. Chim. Acta* **291,** 137–155

73. González, L. O., Pidal, I., Junquera, S., Corte, M. D., Vázquez, J., Rodríguez, J. C., Lamelas, M. L., Merino, A. M., García-Muñiz, J. L., and Vizoso, F. J. (2007) *Br. J. Cancer* **97,** 957–963

74. Vizoso, F. J., González, L. O., Corte, M. D., Rodríguez, J. C., Vázquez, J., Lamelas, M. L., Junquera, S., Merino, A. M., and García-Muñiz, J. L. (2007) *Br. J. Cancer* **96,** 903–911

75. Nannuru, K. C., Futakuchi, M., Varney, M. L., Vincent, T. M., Marcusson, E. G., and Singh, R. K. (2010) *Cancer Res.* **70,** 3494–3504

76. Dean, R. A., Butler, G. S., Hamma-Kourbali, Y., Delbé, J., Brigstock, D. R., Courty, J., and Overall, C. M. (2007) *Mol. Cell. Biol.* **27,** 8454–8465

77. Dean, R. A., and Overall, C. M. (2007) *Mol. Cell. Proteomics* **6,** 611–623

78. Tam, E. M., Morrison, C. J., Wu, Y. I., Stack, M. S., and Overall, C. M. (2004) *Proc. Natl. Acad. Sci. U.S.A.* **101,** 6917–6922

79. Butler, G. S., Dean, R. A., Tam, E. M., and Overall, C. M. (2008) *Mol. Cell. Biol.* **28,** 4896–4914

80. Roemisch, J., Gray, E., Hoffmann, J. N., and Wiedermann, C. J. (2002) *Blood Coagul. Fibrinolysis* **13,** 657–670

81. Lafleur, M. A., Hollenberg, M. D., Atkinson, S. J., Knäuper, V., Murphy, G., and Edwards, D. R. (2001) *Biochem. J.* **357,** 107–115

82. Chen, H. T., Tsou, H. K., Tsai, C. H., Kuo, C. C., Chiang, Y. K., Chang, C. H., Fong, Y. C., and Tang, C. H. (2010) *J. Cell. Physiol.* **223,** 737–745

83. Radjabi, A. R., Sawada, K., Jagadeeswaran, S., Eichbichler, A., Kenny, H. A., Montag, A., Bruno, K., and Lengyel, E. (2008) *J. Biol. Chem.* **283,** 2822–2834

84. Koo, B. H., Park, M. Y., Jeon, O. H., and Kim, D. S. (2009) *J. Biol. Chem.* **284,** 23375–23385

85. Orbe, J., Rodríguez, J. A., Calvayrac, O., Rodríguez-Calvo, R., Rodríguez, C., Roncal, C., Martínez de Lizarrondo, S., Barrenetxe, J., Reverter, J. C., Martínez-González, J., and Páramo, J. A. (2009) *Arterioscler. Thromb. Vasc. Biol.* **29,** 2109–2116

86. Yang, C. M., Hsieh, H. L., Yao, C. C., Hsiao, L. D., Tseng, C. P., and Wu, C. B. (2009) *J. Biol. Chem.* **284,** 26040–26050

87. Knäuper, V., Smith, B., López-Otin, C., and Murphy, G. (1997) *Eur. J. Biochem.* **248,** 369–373

88. Bar-Shavit, Z. (2007) *J. Cell. Biochem.* **102,** 1130–1139

89. Nam, J. S., Kang, M. J., Suchar, A. M., Shimamura, T., Kohn, E. A., Michalowska, A. M., Jordan, V. C., Hirohashi, S., and Wakefield, L. M. (2006) *Cancer Res.* **66,** 7176–7184

90. Qian, B. Z., Li, J., Zhang, H., Kitamura, T., Zhang, J., Campion, L. R., Kaiser, E. A., Snyder, L. A., and Pollard, J. W. (2011) *Nature* **475,** 222–225

91. Li, X., and Eriksson, U. (2003) *Cytokine Growth Factor Rev.* **14,** 91–98

92. Katagiri, T., and Takahashi, N. (2002) *Oral. Dis.* **8,** 147–159

93. Roodman, G. D. (2004) *N. Engl. J. Med.* **350,** 1655–1664

94. Fong, S. T., Camakaris, J., and Lee, B. T. (1995) *Mol. Microbiol.* **15,** 1127–1137

95. Navaratnam, D. S., Fernando, F. S., Priddle, J. D., Giles, K., Clegg, S. M., Pappin, D. J., Craig, I., and Smith, A. D. (2000) *J. Neurochem.* **74,** 2146–2153

96. Perrier, A. L., Cousin, X., Boschetti, N., Haas, R., Chatel, J. M., Bon, S., Roberts, W. L., Pickett, S. R., Massoulié, J., Rosenberry, T. L., and Krejci, E. (2000) *J. Biol. Chem.* **275,** 34260–34265

97. Perrier, A. L., Massoulié, J., and Krejci, E. (2002) *Neuron* **33,** 275–285

98. Yang, J., Yang, H., Yan, L., Yang, L., and Yu, L. (2009) *Mol. Biol. Rep.* **36,** 63–69

99. Naylor, M. J., Oakes, S. R., Gardiner-Garden, M., Harris, J., Blazek, K., Ho, T. W., Li, F. C., Wynick, D., Walker, A. M., and Ormandy, C. J. (2005) *Mol. Endocrinol.* **19,** 1868–1883

100. Butler, G. S., and Overall, C. M. (2009) *Nat. Rev. Drug Discov.* **8,** 935–948

101. Lynch, C. C., Vargo-Gogola, T., Martin, M. D., Fingleton, B., Crawford, H. C., and Matrisian, L. M. (2007) *Cancer Res.* **67,** 6760–6767

102. Schneeweis, L. A., Willard, D., and Milla, M. E. (2005) *J. Biol. Chem.* **280,** 41155–41164